COST-EFFICIENT BATHYMETRIC MAPPING USING SENTINEL DATA

Caleb Olutayo OLUWADARE and Emmanuel Tolulope SANYAOLU (Nigeria)

Summary

The high cost associated with traditional bathymetric survey, high resolution imagery such as IKONOS and insufficient/lack of up-to-date bathymetric charts of most areas in Nigeria calls for a pragmatic and urgent intervention. This study adopts a ratio-transform algorithm on Sentinel-2A imageries for a period of five years (2016 and 2020). Spatio temporal changes along Opa Dam bed were determined from the bathymetric data obtained from Sentinel-2A imageries. Cross-sections and profile along the water channel of the dam were generated. This study offers a new method to provide an accurate depth map while reducing cost up to 75%. Cloud-free Sentinel-2A (Level1) images for 5 years (2016-2020) were downloaded from United States Geological Survey (USGS) Earth Explorer's and Global Land Cover Facility's (GLCF) websites. Water/land separation was done using QGIS 3.10. Stumpf's algorithm was used to determine the Bathymetric Ratio of Blue/Green Bands. Digitization was carried out along the profile and cross sections of the dam bed. Spatio-temporal variation of the dam bed was determined. Analysis of the average BathyRatio depth (ratio of reflectance of Blue and Green bands) and the net change between 2016-2020 were also determined. The result showed that the deepest value along the channel was recorded in 2016. Gradual accumulation of silt at the base continued till 2018 with 1.043 as the value. Between 2018-2020, maintenance activities were suspected. Average BathyRatio for the period was lowest in 2017 (0.990) and the highest was 1.129. The use of Sentinel data provides a cost-effective methodology for estimating water depth and mapping.

Keywords: Bathymetry, Sentinel, Cost-Efficiency, Dam, Remote Sensing.

1. BACKGROUND TO THE STUDY

In the recent time, there has been a great demand for up-to-date bathymetric and topographic maps of shallow water areas and adjacent beaches for creation of nautical charts to guarantee public safety, commerce and the prevention of human and environmental disasters. Bathymetry is essential for various types of applications and studies which include: Coastal flood forecasting, erosion forecasting, coastal defence, the monitoring of morphological changes, the identification of shoreline erosion or accretion, navigation, and fishing (Salameh *et al*., 2019).

It also helps in determining the existing status of the water body; to ascertain the dredged volume for sedimentation purposes, to verify for erosion or accretion, pre and post dredging bathymetry.

Bathymetry is the science that involves measurement of the depth of water bodies as well as the determination of positions with respect to a datum. It involves the acquisition of geometric information of the sea bed for the depiction of underwater topography (Olayinka & Okolie, 2017). Bathymetry serves greatly in enhancing the identification of likely features on the seabed such as elevation changes, rock outcrop, wreck-ages, sunken vessels, pipeline, or any other obstructions that could cause hazard to navigators (Ekpa & Abasiekong, 2018).

Means of collecting bathymetric data over the years include sounding line, single-beam sonar, multi-beam echo sounder, side scanning sonar. The techniques for measuring depth using vehicles ranging from near-bottom remotely operated vehicles to ships on the sea surface to satellites in the space (Olayinka & Okolie, 2017). These vehicles and systems use any of acoustic, optics and radar altimetry to measure bathymetry directly or indirectly.

Mason *et al*. (2000) noted that conventional techniques, such as ground, ship-borne, and airborne-based surveying give very accurate measurements. Multi-Beam Echo Sounders (MBES) are designed originally for deep water measurements, and now are commonly being used for high resolution bathymetry retrieval in near shore areas, as well as surveys in challenging tidal environments (Porskamp *et al.*, 2018). Although, recent developments, as documented by Madricardo *et al.* (2017) have enabled the use of MBES in up to 1 m depths with resolutions reaching 0.05 m. Nonetheless, these techniques are better suitable for relatively small areas and are limited by logistical difficulties and high costs (Mason *et al*., 2000).

There are several satellite-based imaging systems available, which include *Systeme Pour l'Observation de la Terre* (SPOT), LandSat-8 Operational Land Imager (OLI), Sentinel-2/MSI (MultiSpectral Instrument), WorldView, Quickbird, IKONOS, Pleiades, ERS-1 and 2, TerraSAR-X and Sentinel-1 among others. From the listed imageries, Landsat and Sentinel are free. Multispectral remote sensing datasets characterized by high spatial and temporal resolutions is the most frequently used method to estimate bathymetry on shallow water bodies such as coastal areas, estuaries, rivers and lakes (Pacheco *et al*., 2015).

Opa dam, situated within Obafemi Awolowo University campus, Ile-Ife, Nigeria, is meant to provide safe drinking water for the university community; thereby contributing to the accomplishment of the Goal 6 of the Sustainable Development Goals (SDGs) of the United Nations – ensure availability and sustainable management of water and sanitation for all. The dam and its surroundings have always been inundated by flood which has often led to underwater changes. Opa dam upstream activities result in debris and silts being deposited as flood-carrying particles are not sufficiently channelled away from the reservoir. This has resulted into the inability of the dam in providing clean and safe water for the community dwellers. Ogunkoya (2012) recommended a regular investigation of Opa dam bottom configuration. Oyekanmi & Mbossoh (2018) noted that floating materials and silts deposits at the spillway minimize dam's storage capacity. It is important to investigate and map these underwater changes in order to adequately salvage the poor water situation.

The common traditional method of mapping water bed using echo sounder is expensive, time consuming and characterized by high risk. A decade ago, Ogunkoya (2012) employed traditional echo sounding approach, associated with high cost to monitor Opa dam bed. Probably, the high cost of modern sounding equipment has prevented regular mapping of the dam as recommended by Ogunkoya (2012). Regrettably, universities in Nigeria are not adequately funded. The traditional method of using echo sounder does not support regular monitoring of the dam bed due to high cost involved, hence alternative approach of satellite bathymetry is needed to monitor the water bed in order to adequately provide for sustainable water provision for the university community. This study is aimed at providing a cost- and time-effective alternative through Sentinel data.

1.1 Study Area

The study area (Figure 1), Opa dam is located between latitude 7º 30′ 06″N to 7º 30′ 54″N and longitude 4º 31′ 41″E to 4º 32′ 07″E within the Obafemi Awolowo University Community, Ile-Ife, Nigeria. In 1978 an earth-fill dam was constructed by the University with a concrete un-gated spillway on the River Opa (Ogunkoya, 2012). The River Opa as documented by Akinbuwa and Adeniyi (1996) cited in Eludoyin *et al.* (2004) has its source from Oke-Opa, a hill along Ife/Ilesha road (Osu area), and a number of rivers (the likes of Rivers Amuta, Obudu and Esinmirin) combine to form this river.

The reservoir at creation was about 2.5km long, with 0.80km at its widest point and has the total surface area of about 0.95 km^2 maximum capacity of about 675,000m^3 (Ogunkoya, 2012). The depth ranges between 1.01m and 4.99m, having a live storage of about 389,000 m^3 at this level said Taiwo *et al*. (2017). The result of successive bathymetric contours carried out by Ogunkoya (2012) shows about 41.4% change in the reservoir’s total volume between 1978 and 2010.

During the dry season the water volume reduces considerably, while in the rainy season, the volume of water inflow increases as a result of floods, causing high turbidity and a general immersion of the vegetation on the shoreline (Adedeji *et al.*, 2018). This seasonal variation in the water release into the reservoir directly affects its water level.

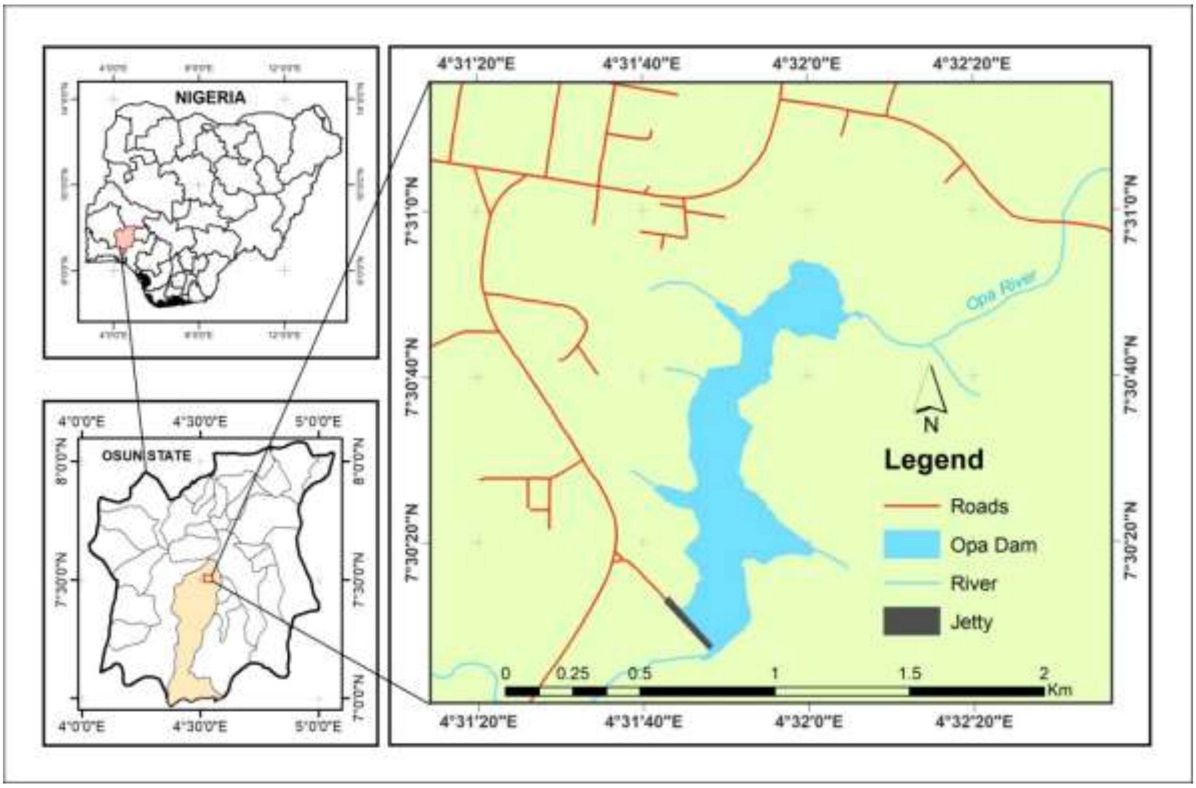

Figure 1: Study Area Map (Source: Authors, 2020)

2. LITERATURE REVIEW

Various methods of collecting bathymetric details exist and these include Boat-based acoustic survey (Hydrographic survey), Airborne LIDAR, Passive Optical Remote Sensing (Jawak *et al*., 2015).

Boat-based acoustic bathymetry

Olayinka and Okolie (2017) observed that hydrographic surveys have been performed from ships and boats using different types of devices, systems and procedures including sounding line (Adediji, 2005), single-beam sonar (Yunus *et al*., 2019), multi-beam echo sounder (Madricardo *et al*., 2017), side scanning sonar (Bai & Bai, 2018). Side scanning sonar is efficient in detecting obstructions on the seafloor that may be hazardous to shipping or to seafloor installations for subsea field development.

Boat-based acoustic bathymetry systems are limited by the operational and logistic difficulties, the number and frequency of surveys performed, high costs and their geographic coverage; particularly in relatively shallow coastal waters where survey swaths are small (Mason et al., 2000; Haibin Su et al., 2008)

Satellite-based Bathymetry

Bathymetric mapping derived from satellites is an alternative method for bathymetric estimation by remote sensing technology that uses electromagnetic radiation (Doxania *et al.*, 2012). By contrast, the approach of remote sensing is faster and applicable to diverse environment like shallow coastal waters and clear rivers (Berk *et al.*, 1998). Remote sensing enables the simulation of bathymetry at spatial scales which cannot be done with conventional methods. The two broad categories used in remote sensing to extract information on the bathymetry are active methods of remote sensing and passive methods of remote sensing (Jawak *et al.*, 2015).

Bathymetry derived from active sensor

Active sensors transmit electromagnetic energy pulses and record the origin and intensity of the backscatter obtained from objects within the field of view of the system, such as synthetic aperture radar (SAR), and light detection and range (LIDAR) (Jawak *et al.*, 2015). Taking measurements in all-weather conditions and any time of the day (day and night) are important benefits of active sensors (Tuell *et al.*, 2005). Active sensors may be used to examine wavelengths that are not effectively supported by the sun and these sensors could be imaging or non-imaging sensors (Park *et al.*, 2010).

The two primary non-imaging active remote sensing methods used for derivation of bathymetry are LIDAR and satellite altimetry (radar altimeters and scatterometers) (Wang & Philpot, 2007). LIDAR as explained by Pastol (2011) is light detection and ranging, measuring the distance between the sensor and the surface of the water or an ocean floor by a single wave pulse or double waves. It is the time drift of the returned radiation pulses at the sensed spots from the object, which is ultimately used to produce bathymetric information. But the uneven bathymetric sampling interval and high cost limit this approach (Park *et al.*, 2010).

RAdio Detection And Ranging (radars) are sensors for imaging. Radar satellites use short electromagnetic radiation pulses within the spectrum of microwaves (Jawak *et al.*, 2015). They are not affected by wind, fog, dust, cloud and bad weather; and are not dependent on the illumination from the sun. These satellites compute the reflected radar pulses from the ground surface; determine the signal strength or intensity to retrieve information about the earth's surface structure, and sort the time elapsed between the pulse emission and return (Jawak *et al.*, 2015). Radar detects backscattered differences from the surface of the water, e.g. roughness induced by wave spectrum modulations in relation to surface current, (Vogelzang *et al.*, 1943).

Bathymetry derived from passive sensor

This is inferred from image pixel values based on changes in intensity of an external source of radiation (e.g. sunlight), emitted (e.g. thermal infrared energy) or reflected (e.g. blue, green, red, and near-infrared light) by the object; in contrast to active sensors used in echo-sounders or LIDAR systems that measure water depth based on the two-way travel time of a well-controlled transmitted signal. (Bierwirth & Burne, 1993; Freire, 2017; Jawak *et al.*, 2015; Yunus *et al.*, 2019).

Different satellite-based imaging systems are available, including free ones (such as Landsat and Sentinel); as well as algorithms/models developed as a result of several studies tailored towards estimation of water depth through remote sensing (El-sayed, 2018). The performance of this method hangs on the quality of the image and the algorithm/model used (Abd-Almajied, 2015).

The algorithms could be physics-based with no need of in-situ depth measurement or empirical/analytical which require in situ depth measurement for calibration. In Kerr & Purkis (2018) study, a bridge was provided between the empirical and physics-based approaches by combining the forward modeling of the water column method of Lee *et al.* (1999) with the ratio algorithm of Stumpf *et al*. (2003). Kerr & Purkis (2018) model allows for the estimation of water depths up to 15 m in tropical carbonate environments with no need of in situ water depth measurements as calibration data. They provided a solution to the challenge of lack of ground-truth data which is often the major obstacle for satellite-derived bathymetry in shallow-water environments. As reported by Kerr & Purkis (2018) a root-mean-squared error of 1.43 m in areas less that 15m depth was achieved when Kerr & Purkis (2018) model was applied to RapidEye imagery from Andros Island. However, some applications require water depth precision to be in tens of centimeters rather than meters (Geyman & Maloof, 2019; Maloof & Grotzinger, 2012), thus the need for a more precise model which could require a set of in-situ data (Geyman & Maloof, 2019). Available in the literature is a number of empirical algorithms (such as Stumpf *et al*. (2003) and Su *et al*. (2008)) and analytical algorithms (such as Lyzenga *et al*. (2006); Lyzenga (1978); Lyzenga, (1985)) for water depth estimation.

Lyzenga (1978; 1985) model has been modified and extensively applied to the bathymetric mapping of shallow water by various researchers, which include works by Clark *et al*. (1987); Kanno *et al*. (2013); Khondoker *et al*. (2016); Liang *et al*. (2017); Lyons *et al*. (2011); Lyzenga *et al*. (2006); Philpot (1989); Sam *et al*. (2018) to mention a few. The algorithm employed in this research in determining water depth from satellite imagery was based on the Beer's Law of Absorption, which proposes a log-linear relationship between reflectance and water depth. However, depth estimates from Lyzenga (1978; 1985) may be biased since a uniform bottom albedo is assumed (Geyman & Maloof, 2019). Also, to measure the performance of the mapping of the bathymetry with Lyzenga model requires a number of input parameters such as properties of atmosphere, bottom material, water column and other parameters (El-sayed, 2018).

In order to put the independence of water bottom condition into consideration in estimating depth of shallow water, studies such as Clark *et al*. (1987); Green *et al*. (2000); Stumpf *et al*. (2003); Kerr & Purkis (2018) among others attempted to use the ratio of reflectance for two different spectral. Since the rate of light attenuation in water depends on wavelength, the ratio of reflectance for two different wavelengths is a function of water depth and, in theory, less sensitive to bottom albedo (Geyman & Maloof, 2019). These algorithms made it clear that the most important bands are blue, and green (El-sayed, 2018). The additional advantage of the empirical method (linear ratio algorithm) is that it requires few parameters which are simple for mapping the bathymetry of shallow water. Hence, the ratio method by Stumpf *et al*. (2003) adopted in this study.

Besides the models for mapping bathymetry, the quality of the satellite image used is also of great importance to ascertain the performance of satellite derived bathymetric method (Abd-Almajied, 2015). The pioneer study on mapping of bathymetry from remote sensing imagery by Lyzenga (1978) was demonstrated using aerial photographs over clear shallow water. The use of passive optical multi-spectral satellite imagery had been widely used by many researchers and such include Landsat (Benny & Dawson, 1983; Deng *et al*., 2008; El-sayed, 2018; Jupp, 1988; Lyzenga, 1981; Lyzenga, 1985; Okolie, 2015; Olayinka & Okolie, 2017; Vinayaraj *et al*., 2016; Yunus *et al*., 2019), IKONOS (Stumpf *et al*., 2003; Su *et al*., 2008), QuickBird (Conger *et al*., 2006; Deng *et al*., 2008; Mishra *et al*., 2006), SPOT (Mohamed *et al*., 2016), RapidEye (Geyman & Maloof, 2019; Kerr & Purkis, 2018; Vinayaraj *et al*., 2016), Sentinel (El-sayed, 2018; Yunus *et al*., 2019) imageries among others. Among these satellites Landsat and Sentinel are the most available to the global user community at no cost. Sentinel was chosen for this study because of its high spatial resolution compare to that of Landsat.

3. RESEARCH METHODOLOGY

The methodological workflow used in this study is as shown in Figure 2.

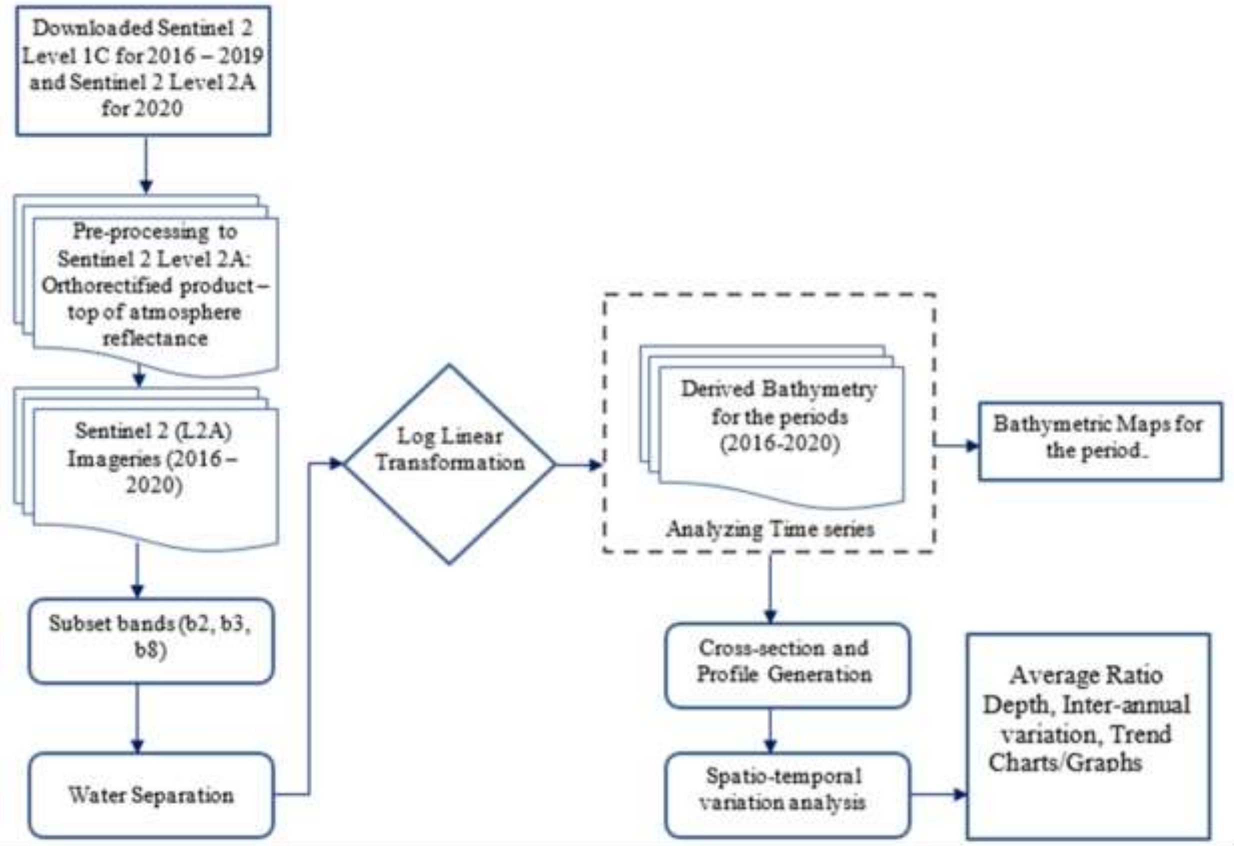

Figure 2: Methodological Workflow
Source: Authors (2020)

3.1 Data Collection

Cloud-free Sentinel-2A Level 1C images of 2016 to 2019 and Sentinel-2A Level 2A (Orthorectified product – top of atmosphere) image for the study area were downloaded from United States Geological Survey (USGS) Earth Explorer's and Global Land Cover Facility's (GLCF) websites. The selection of these images was based on the percentage of cloud cover, date of acquisition, spatial resolution and cost. The details of the satellite data acquired are shown in Table 1

Table 1: Satellite imageries used in this study and the source

Sensor	Date of Acquisition	Time of Acquisition (HH:MM:SS)	Bands used	Band Resolution	Source
Sentinel-2A (Level 1C)	07-01-2016	10:12:36	Band 2 – Blue, Band 3 – Green, Band 8 – Near Infrared (NIR)	10	USGS Earth Explorer website
Sentinel-2A (Level 1C)	01-01-2017	10:11:20	Band 2 – Blue, Band 3 – Green, Band 8 – Near Infrared (NIR)	10	USGS Earth Explorer website
Sentinel-2A (Level 1C)	16-01-2018	10:16:29	Band 2 – Blue, Band 3 – Green, Band 8 – Near Infrared (NIR)	10	USGS Earth Explorer website
Sentinel-2A (Level 1C)	11-01-2019	10:14:28	Band 2 – Blue, Band 3 – Green, Band 8 – Near Infrared (NIR)	10	USGS Earth Explorer website
Sentinel-2A (Level 2A)	16-01-2020	10:03:41	Band 2 – Blue, Band 3 – Green, Band 8 – Near Infrared (NIR)	10	USGS Earth Explorer website

3.2 Derivation of Bathymetry from Sentinel-2A

A number of factors affect the state of the atmosphere (e.g., haze, aerosols, and clouds), sea surface (e.g., sun glint, sky glint, and white caps) and water column (e.g., sedimentation, turbidity and variable optical properties) affecting the remote sensing of the optically shallow extent (where part of the water surface remote signal contains a bottom signal). So, the atmospheric and radiometric correction (converting image from the digital number to the top of atmosphere (TOA) spectral radiance values) of the images were first carried out using Semi-Automatic Classification Plugin in QGIS. This is required to obtain Bottom of Atmosphere (BOA) reflectance images derived from the Level-1C products. Land and water were separated and the depth derived as explained in the subsections.

3.2.1 Water Separation

Dry land on the images was removed and the water threshold values for the image scene were determined. This was done by digitizing a line on the image extending from the land portion across the waters on the NIR band (band 8). A profile graph to display the change in reflectance value with respect to distance along the digitized line created using Profile Tool Plugin in QGIS 3.10 as shown in Figure 3.

The land area often has higher surface reflectance and this could be observed by a sharp drop in the profile line occurring at the land/water intersection when the line touched the areas covered by water. The water threshold value was recorded at this sharp drop which indicates the land/water separation zone. The sections having low values and high values represent water and land respectively.

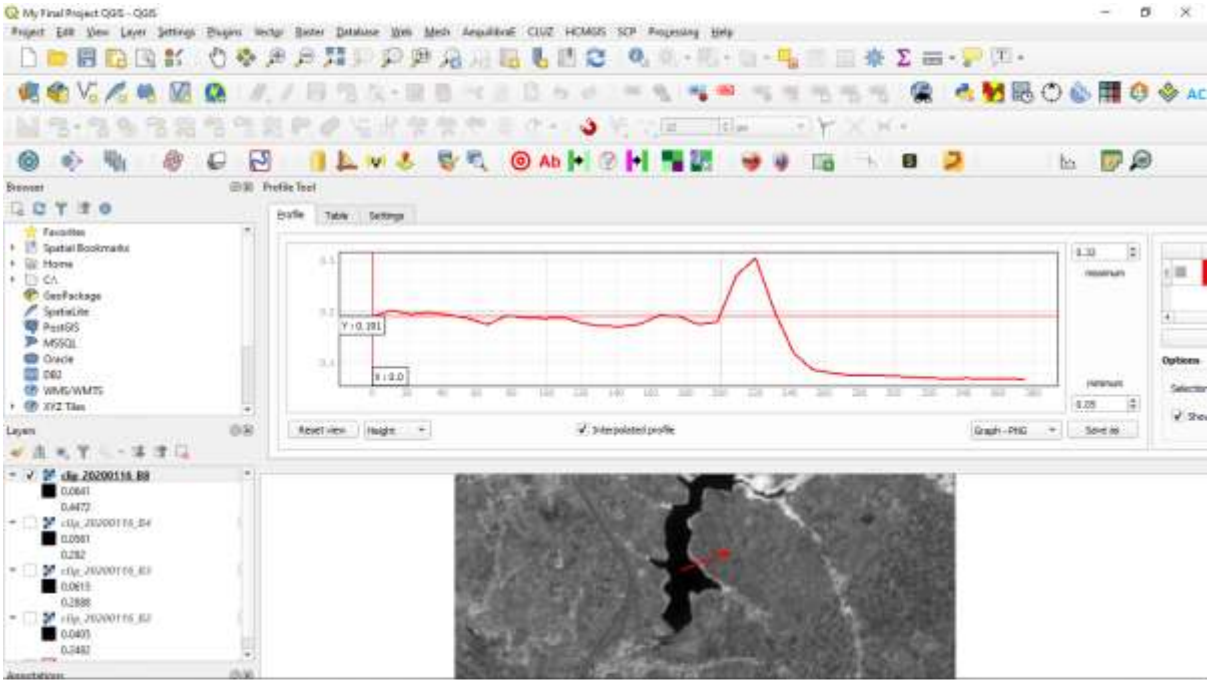

Figure 3: Creating profile graph using Profile Tool Plugin in QGIS 3.10

The water threshold values for the years in consideration are presented in Table 2.

Table 2: Values for Land/Water threshold

Sentinel Data	Date of Acquisition	Water Threshold Values (Surface Reflectance)
Sentinel-2A	07-01-2016	0.108
Sentinel-2A	01-01-2017	0.079
Sentinel-2A	16-01-2018	0.048
Sentinel-2A	11-01-2019	0.064

Sentinel-2A	16-01-2020	0.112

Using Raster Calculator in QGIS 3.10, a set of queries was written to eliminate the portion of land from water in the blue and green bands required for the years under consideration. A sample query is shown as follows:

For Blue band: ("clip_20160107_B8" < 0.108) * "clip_20160107_B2"

For Blue band: ("clip_20160107_B8" < 0.108) * "clip_20160107_B3"

Where "clip_20160107_B8" is the Near Infrared Band of year 2016, 0.108 is the water threshold value, "clip_20160107_B2" is the Blue Band and "clip_20160107_B3" is the Green Band.

3.2.2 Depth Derivation

Stumpf's algorithm $Z = m_1 \frac{\ln(n*Rw(\lambda i))}{\ln(n*Rw(\lambda j))} - m_0$, was used to determine the bathymetry, which involves calculation of gain (m_1) and offset (m_0) for referencing the algorithm result to the chart datum. Stumpf's algorithm takes the form of straight-line equation, $y = m_1x – m_0$ where m_1 is a tuneable constant to scale the ratio to depth, n is a fixed constant for all areas to assume that the algorithm is positive, and m_0 depth is the offset for a depth of 0m where depth, Z=0. Rw is the reflectance of water, and (λi, j) are two different bands (blue and green respectively).

Due to lack of reference data, this study was limited to 'Ratio Depth' by calculating the independent variable in Stumpf's algorithm $\frac{\ln(n*Rw(\lambda i))}{\ln(n*Rw(\lambda j))}$ referred to as BathyRatio in this study using Raster Calculator in QGIS 3.10. The Raster Calculator expression is shown in Eq. 1

BathyRatio = In([Blue])/In([Green]) … Eq. 1

So, the Ratio Depth (BathyRatio) was generated for the years in consideration.

3.3 Temporal Changes

A profile was generated along the centerline of the Dam channel to examine the changes that had occurred between 2016 and 2020, considering the average depth, net change and trend. This was done by digitizing a line along the centre of the water channel of the dam using year 2020 image as the reference image. This line was taken as a profile line for the images from 2016 to 2020. The BathyRatio depths derived were added to QGIS environment and the digitized line was also added. The profile data was automatically generated in QGIS using Terrain Profile of the Profile Tool Plugin (Figure 4) and the data for each year was exported along with their coordinates into excel recognized format (.csv). The profile for each of the periods was then plotted in Excel using Chart (Graph).

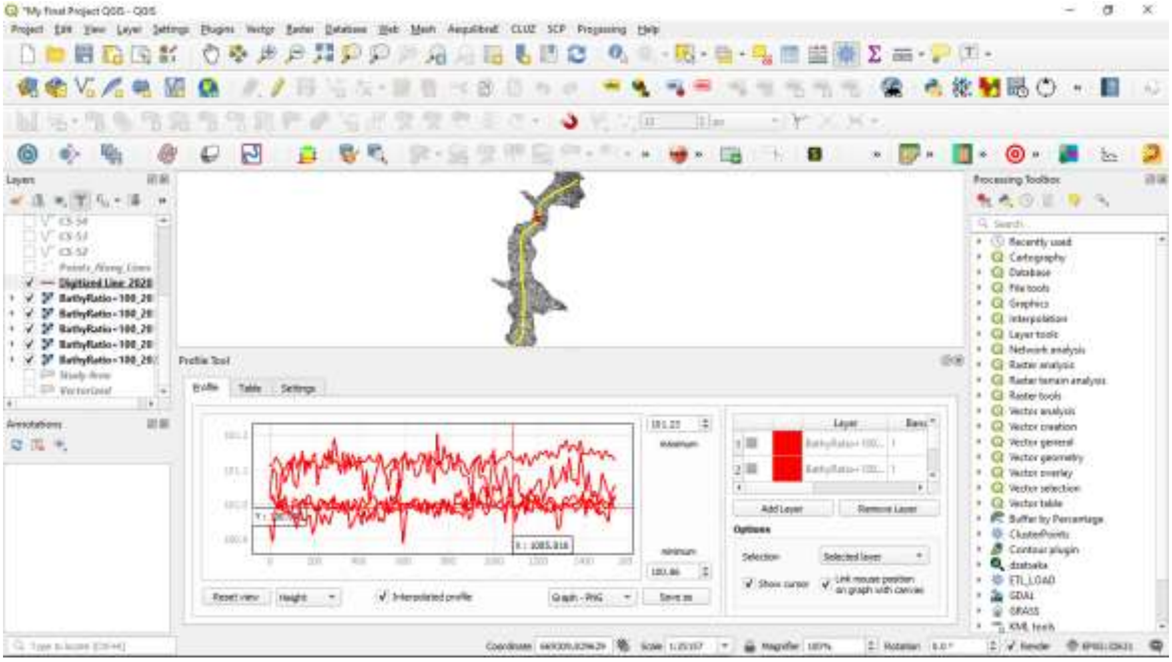

Figure 4: Profile generation in QGIS using Terrain Profile of the Profile Tool Plugin

The same procedures used in generating profile were repeated for cross sections. The only difference was that instead of the digitized line created at the centre of the water channel for profile, three lines were created across the channel, one at the beginning, one at the middle and the last at the end of the channel. Terrain Profile in Profile Tool Plugin of QGIS 3.10, was also used to generate the cross sections for all the years. The cross-section data for each of the lines and periods were exported along with their coordinates into excel format as done for profile. The cross sections were then plotted in Microsoft Excel.

3.3.1 Rate of Spatio-Temporal Variation of the Dam Bed

The profile and cross section information generated were further analyzed in Microsoft Excel and SPSS (Statistical Package for the Social Sciences). From the Profile information the following analysis were carried out:

- Average BathyRatio Depth Graph for each period in consideration were generated in Microsoft Excel 2016.
- The BathyRatio Depth Net Change Chart between 2016 & 2017, 2017 & 2018, 2018 & 2019, and 2019 & 2020 produced in Microsoft Excel 2016 by finding the depth difference between previous and current year, then plotting the differences.
- Trend over time – from 2016 to 2020.

4. DATA PRESENTATION AND DISCUSSION OF FINDINGS

4.1 Depth determination

The results of water separation and derivation of bathymetry in determination of the depth of Opa Dam are presented as follows:

4.1.1 Water Separation

The sample results of the water separation for band 2 and band 3 are presented in Figure 5 & 6 respectively for year 2016. The black portion has value '0' indicating the areas which are not water and the other portion are the areas of the dam having water.

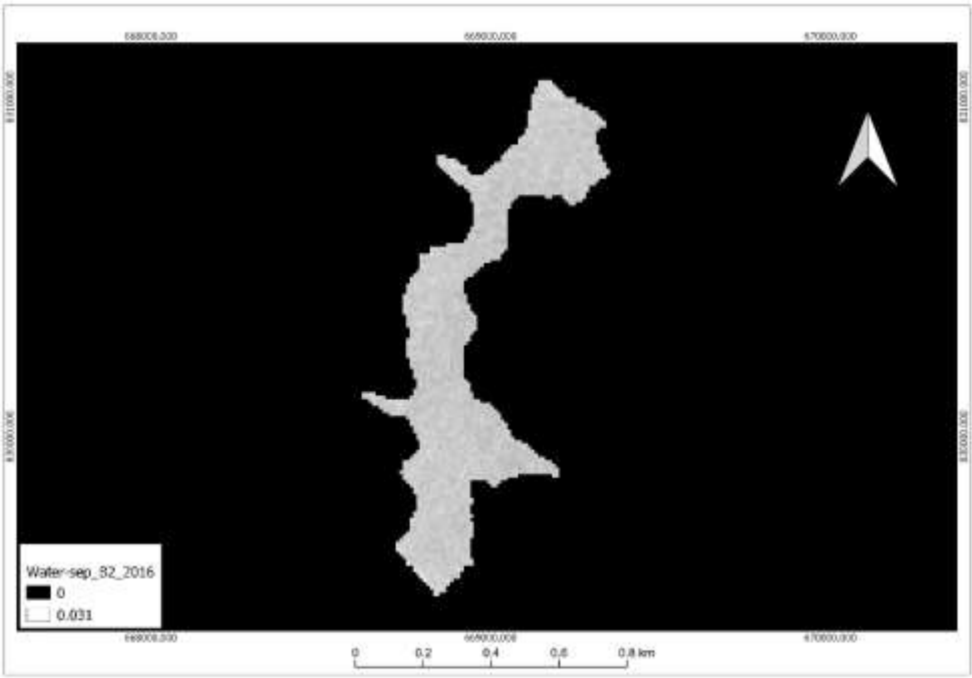

Figure 5: Band 2 (Blue) Water Separation for 2016

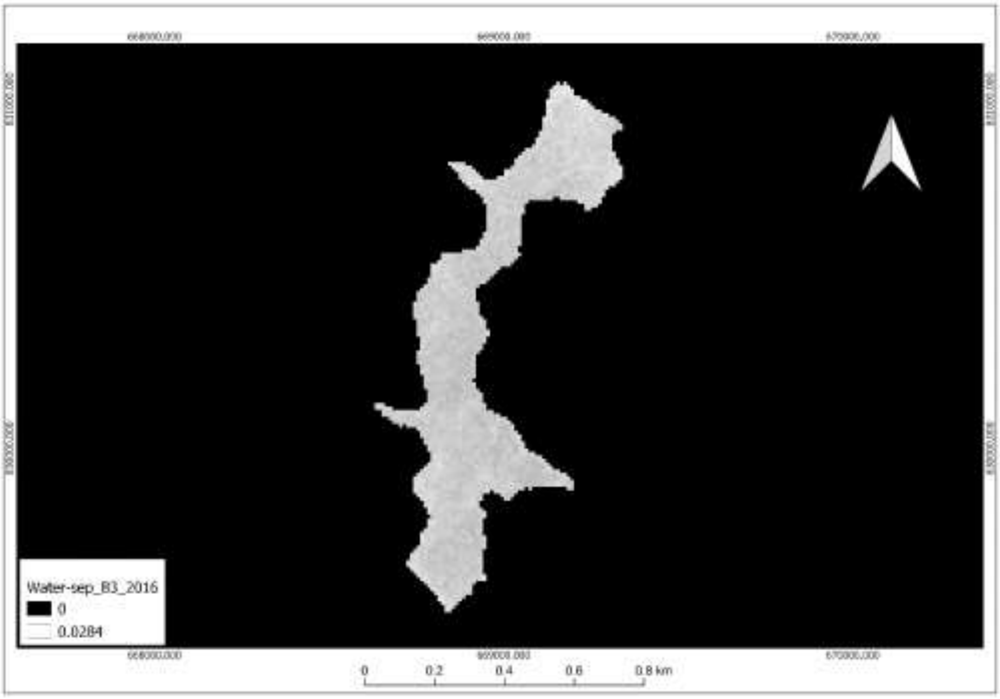

Figure 6: Band 3 (Green) Water Separation for 2016

4.1.2 Derivation of Bathymetry

The bathymetry was derived using Stumpf's algorithm and due to lack of reference data *'Ratio Depth'* (referred to as BathyRatio in this study) alone was obtained without tuning it to actual depth. The results are presented in Figure 7 and Table 3 for the five years.

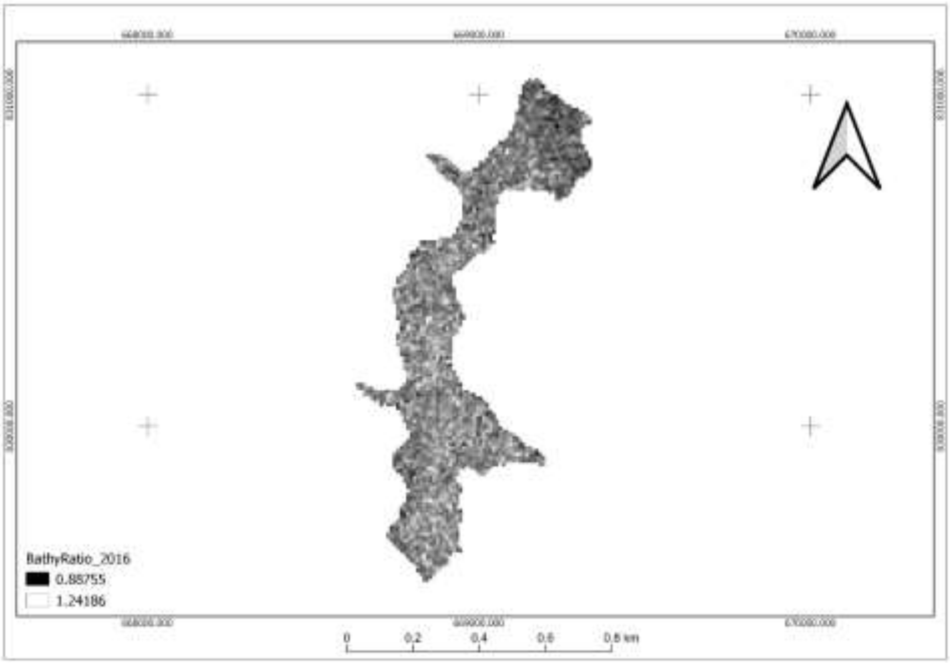

Figure 7: 2016 BathyRatio

Table 3: BathyRatio between 2016 and 2020 in Tabular Form

Year	**2016**	**2017**	**2018**	**2019**	**2020**
Shallow	0.88755	0.856757	0.955587	0.946289	1.06478
Deep	1.24186	1.12094	1.04306	1.05746	1.19638

Figure 7 shows the map for only Year 2016, while other years are summarized in Table 3. The results as presented in Figure 7 and Table 3 show the depth values in ratio of the blue band surface reflectance to green band surface reflectance (not metric unit). The results did not show the actual depth, but variation can be noticed in the results. The BathyRatio for 2016 - 2020 as shown in Table 3 are having ratio depth (ratio of reflectance of blue and green bands) ranging from 1.04306 to 1.241861 and the shallow surface from 0.856757 to 1.06478. The surface reflectance indicates significant variation in the longitudinal profile of the dam.

4.2 Temporal Changes

4.2.1 Average BathyRatio Depth

The results of the graphs of the average ratio depth plotted in Microsoft Excel for the Year 2016 to 2020 are presented in Figure 8 and Table 4.

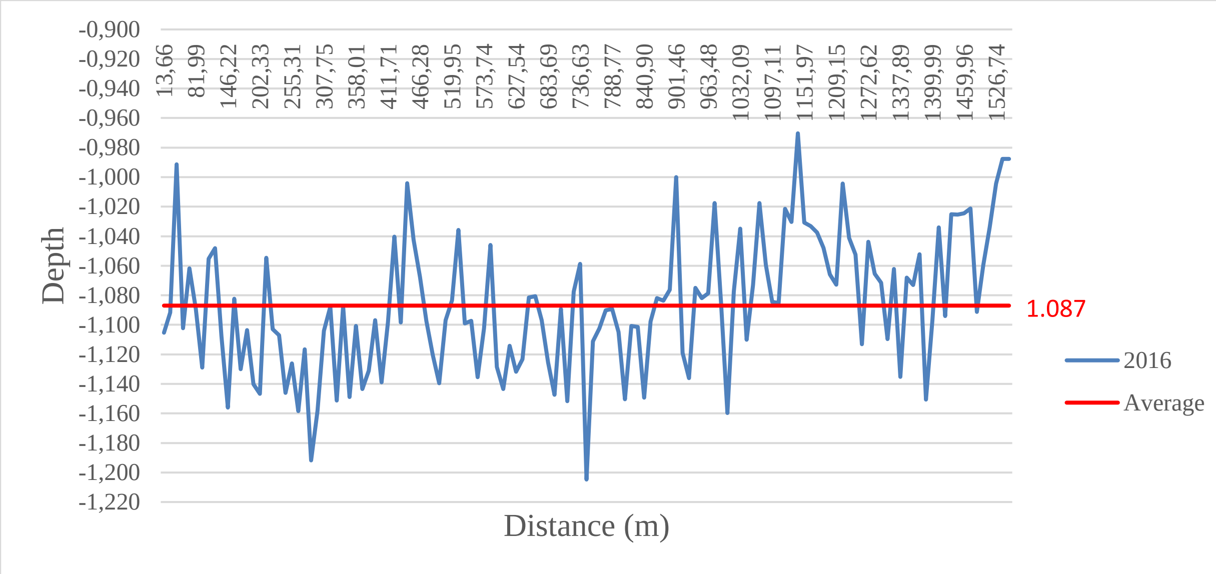

Figure 8: Profile with Average BathyRatio Depth 2016

Table 4: Average BathyRatio Depth between 2016 and 2020 in Tabular Form

YEAR	***2016***	***2017***	***2018***	***2019***	***2020***
AVERAGE BATHYRATIO DEPTH	***1.087***	***0.990***	***1.001***	***0.994***	***1.129***

As shown in Table 4, the average BathyRatio depths for the period between 2016 and 2020 are 1.087, 0.990, 1.001, 0.994 and 1.129. These results indicate that the dam channel depth was deepest in 2020 having a value of 1.129. For a period of 3 years (2017 -2019), there were variations in the depth as well but not well pronounced. Though, this research has the limitation of determining the actual variation in silt accumulation volume due to lack of baseline data, yet the result is justified in the fact that occurrence of variation in the configuration of the waterbed is evident as indicated.

4.2.2 The BathyRatio Depth Net Change Charts between 2016 & 2017, 2017 & 2018, 2018 & 2019, and 2019 & 2020

The BathyRatio depth net change charts showed the changes that occurred over the years. Figures 9 to 12 show the BathyRatio depth net change chart between 2016 & 2017, 2017 & 2018, 2018 & 2019, and 2019 & 2020 respectively. It was clear from the net change chart (Figure 12) that the largest portion of the sampled profile depths were deeper in 2016 than 2017. In Figures 10 and 11, 2018 depths were deeper than 2017 and 2019 respectively. There were deeper depths in 2020 than 2019, as shown in Figure 12. These results indicate that there were changes every two years.

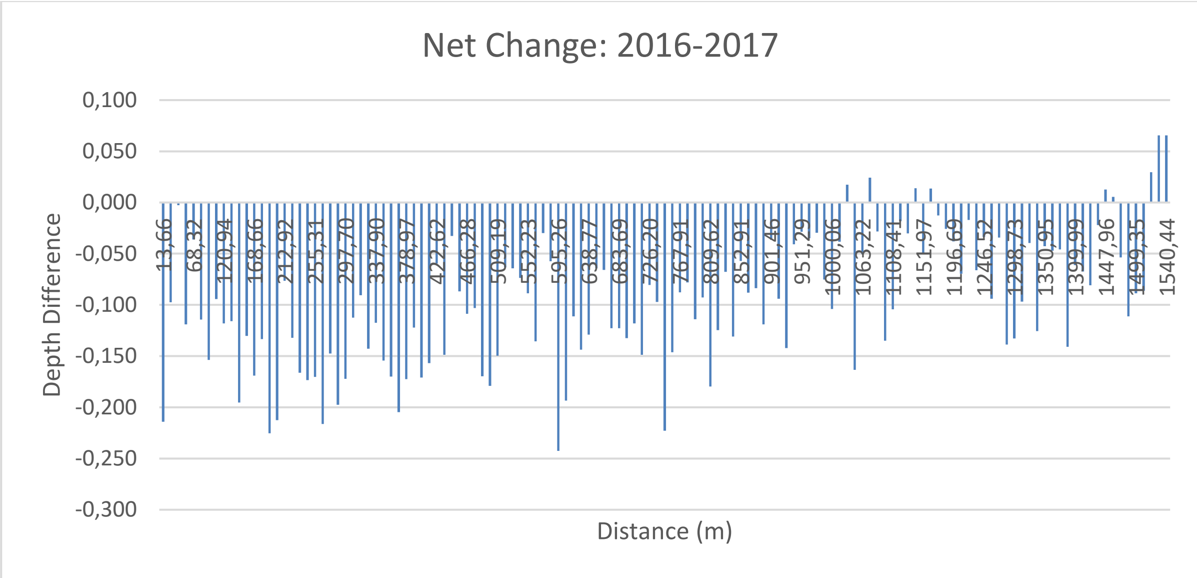

Figure 9: BathyRatio Depth Net Change Chart (2016 – 2017)

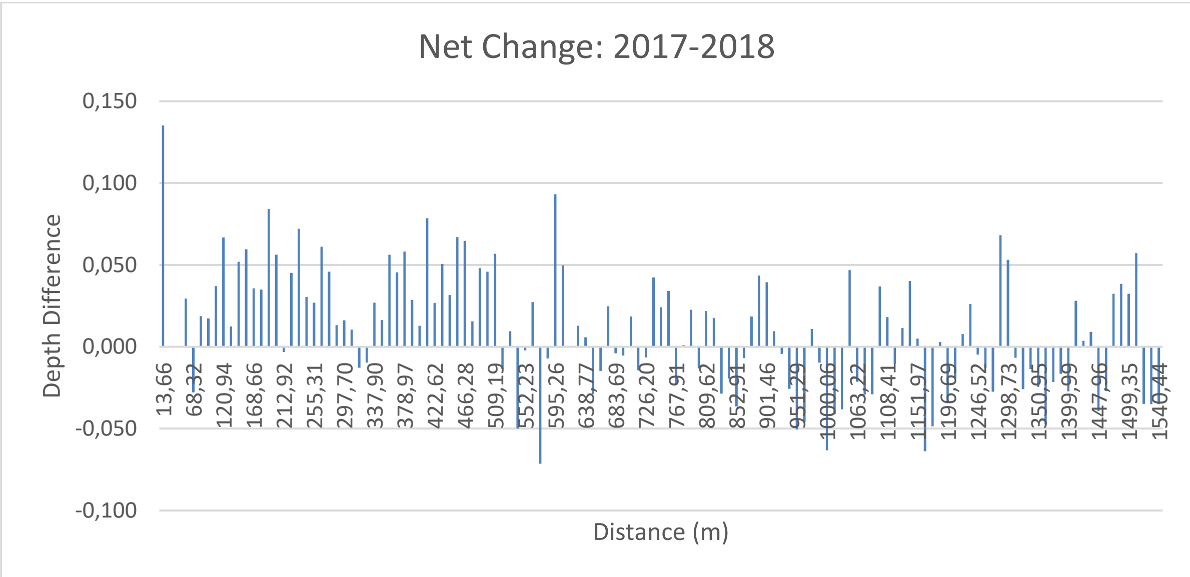

Figure 10: BathyRatio Depth Net Change Chart (2017 – 2018)

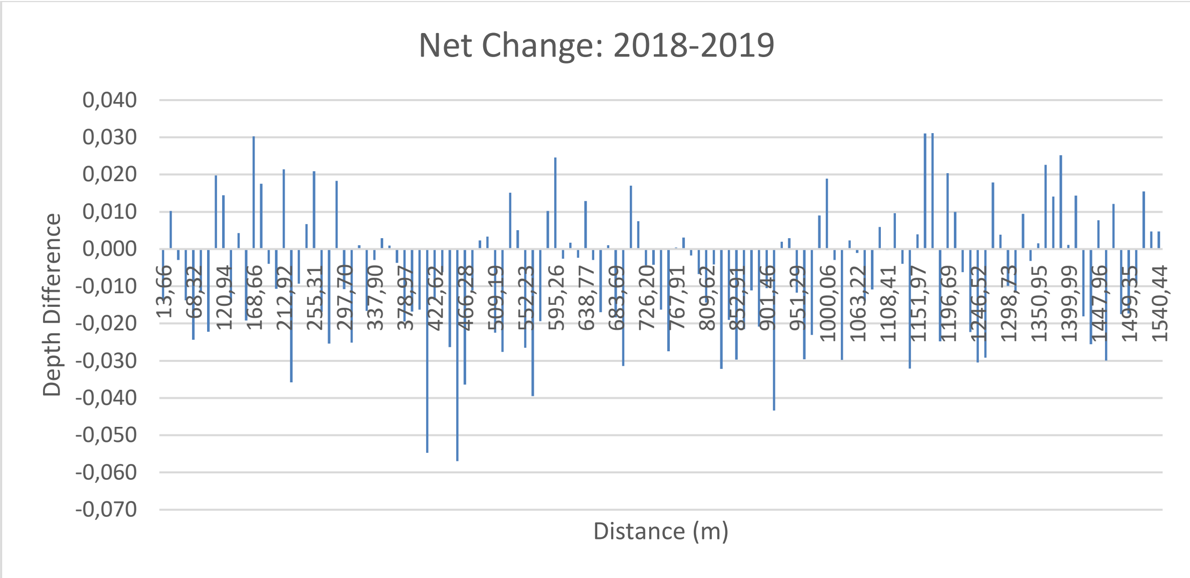

Figure 11: BathyRatio Depth Net Change Chart (2018 – 2019)

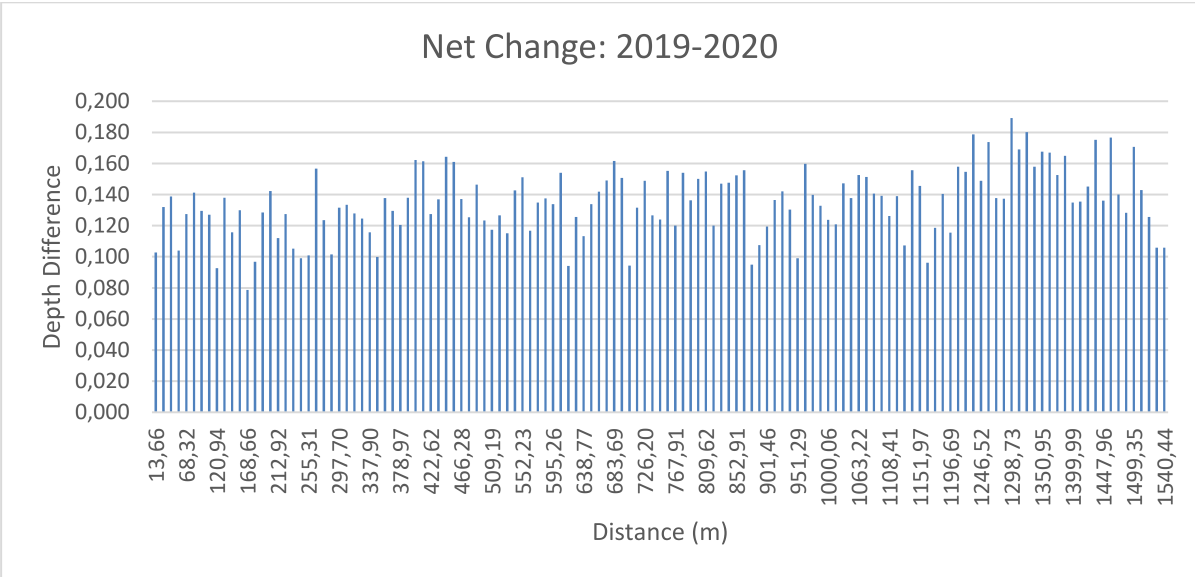

Figure 12: BathyRatio Depth Net Change Chart (2019 – 2020)

4.2.3 Trend over time – from 2016 to 2020

The results of the BathyRatio depth trend shown in Figure 13 confirm the changes along the dam channel over the years and this can be seen at glance vis-a-vis the profile for each year. It can be noticed that the 2016 and 2020 depths are deeper compare to others. It could also be seen that there was a great difference in depth between 2016 and 2017 at the beginning of the channel (around 95.65m) along the profile till it gets to about 422.62m where the difference became a bit minimal before it increased again from chainage 584.50m to 904.23m. A uniform undulation was noticed in the figure between 2018 and 2019. The changes between their depths appeared to be small. On the other hand, there was a great difference in depth all through the channel of the dam along the profile between 2019 and 2020. It is also worthy of note that although 2016 and 2020 depths are deeper compared to others, nonetheless there was a consistent depth variation in 2020 depth along the profile while the depth variation along the channel in 2016 is irregular probably due to routine maintenance on the dam between the year 2017 to 2020 which was not the case before the year 2016. This irregularity could also be seen clearly in 2017 depth (Figure 13) which was not the case in 2018 and 2019. There is need to further investigate the randomness or otherwise of the maintenance activities on the dam between 2017 and 2020 that could have resulted into the sudden and significant changes in the chart.

Figure 13: BathyRatio Depth Trend from 2016 to 2020

5. CONCLUDING REMARKS

The study examined alternative means of mapping waterbed. The cost of bathymetry using acoustic gadgets and other logistics do not guarantee a sustainable maintenance of dam and provision of safe water to university community dwellers. Records from the maintenance department of the university did not suggest any recent sounding activities on the dam. Though record of dredging activities within the specified period (2016-2020) of this research, was not available as at the time of carrying out this research, the Bathyratio analysis suggests that there were noticeable changes at the waterbed configuration which was the intent of this research. The research concluded that using Sentinel-2A data is economical, faster and efficient for the mapping of seabed at little or no cost. Based on the necessity to provide safe drinking water for the teeming population of the university, this study recommends a regular monitoring of the dam on annually basis in order to enhance decisions to be taken on maintenance of the dam and provision of potable water for the university community. Also, it is recommended that further investigation should be carried out on the dam to determine the volume of accretion at the dam bed in order to know the cost implication of dredging and other maintenance works.

REFERENCES

Abd-Almajied, M. (2015). Predicting Water Depth of Lake Using Remote Sensing image. *Iraqi Journal of Science*, *56(2A)*, 1208–1215.

Adedeji, A. A., Bolawa, O. P., & TTaiwo, Y. F. (2018). Ecological Status of Opa Reservoir, Obafemi Awolowo University, Ile Ife, based on the Abundance and Diversity of its Planktonic Flora. *Notulae Scientia Biologicae*, *10*(2), 287–296. https://doi.org/10.15835/nsb10210248

Adediji, A. (2005). Reservoir sedimentation: The case of the opa reservoir catchment, southwestern nigeria. *South African Geographical Journal*, *87*(2), 123–128. https://doi.org/10.1080/03736245.2005.9713835

Bai, Y., & Bai, Q. (2018). *Subsea Engineering Handbook* (Second Edi). Elsevier Inc. https://doi.org/https://doi.org/10.1016/C2016-0-03767-1

Benny, A. H., & Dawson, G. J. (1983). Satellite imagery as an aid to bathymetric charting in the Red Sea. *The Cartographic Journal*, *20*, 5–16.

Berk, A., Bernstein, L. S., Anderson, G. P., Acharya, P. K., Robertson, D. C., Chetwynd, J. H., & Adler-Golden., S. M. (1998). MODTRAN cloud and multiple scattering upgrades with application to AVIRIS. *Remote Sensing OfEnvironment*, *65*, 367–375.

Bierwirth, P., & Burne, R. V. (1993). Shallow sea-floor reflectance and water depth derived by unmixing multispectral imagery. *Photogrammetric Engineering & Remote Sensing*, *59(3)*, 331–338.

Clark, R. K., Fay, T. H., & Walker, C. L. (1987). Bathymetry calculations with Landsat 4 TM imagery under a generalised ratio assumption. *Applied Optics*, *26(19),* 4036–4038.

Conger, C. L., Hochberg, E. J., Fletcher, C. H., & Atkinson, M. J. (2006). Decorrelating remote sensing color bands from bathymetry in optically shallow waters. *IEEE Transactions on Geoscience and Remote Sensing*, *44*, 1655–1660.

Deng, Z., Ji, M., & Zhang, Z. (2008). Mapping Bathymetry from Multi-source Remote Sensing Images: A Case Study in Beilun Estuary, Guangxi, China. *The International Archives of the Photogrammetry, Remote Sensing and Spatial Information Sciences, Vol. XXXVI*(Part B8), 1321–1326.

Doxania, G., Papadopouloua, M., Lafazania, P., Pikridasb, C., & Tsakiri-Strati, M. (2012). Shallow-water bathymetry over variable bottom types using multispectral Worldview-2 image. *International Archives of the Photogrammetry, Remote Sensing and Spatial Information Sciences, XXXIX-B8.*

Ekpa, A., & Abasiekong, I. (2018). *Bathymetric Investigation of Seabed Topographical Changes of Woji Creek*. *9*(11), 1366–1372.

El-sayed, M. S. (2018). Comparative Study of Satellite Images Performance in Mapping Lake Bathymetry : Case Study of Al-Manzala. *American Journal of Geographic Information System 2018*, *7*(3), 82–87. https://doi.org/10.5923/j.ajgis.20180703.02

Eludoyin, A. O., Ofoezie, I. E., & Ogunkoya, O. O. (2004). The effect of Oja-titun market effluent on the chemical quality of receiving OPA reservior in Ile-ife, Nigeria. *Journal of Environmental Management*, *72*(4), 249–259. https://doi.org/10.1016/j.jenvman.2004.05.005

Freire, R. R. (2017). *Evaluating Satellite Derived Bathymetry in Regard To Total Propagated Uncertainty , Multi- Temporal Change Detection , and Multiple Non-Linear Estimation Evaluating Satellite Derived Bathymetry in Regard*.

Geyman, E. C., & Maloof, A. C. (2019). A Simple Method for Extracting Water Depth From Multispectral Satellite Imagery in Regions of Variable Bottom Type. *Earth and Space Science*, *6*(3), 527–537. https://doi.org/10.1029/2018EA000539

Green, E. P., Mumby, P. J., Edwards, A. J., & Clark, C. D. (2000). Remote Sensing Handbook for Tropical Coastal Management. *Coastal Management Sourcebooks 3, January 2000*, x + 316.

Jawak, S. D., Vadlamani, S. S., & Luis, A. J. (2015). A Synoptic Review on Deriving Bathymetry Information Using Remote Sensing Technologies: Models, Methods and Comparisons. *Advances in Remote Sensing*, *04*(02), 147–162. https://doi.org/10.4236/ars.2015.42013

Jupp, D. L. B. (1988). Background and Extensions to Depth of Penetration (DOP) Mapping in Shallow Coastal Waters. *Proceedings of the Symposium on Remote Sensing of the Coastal Zone, Gold Coast*, IV2(1)-IV2(19).

Kanno, A., Tanaka, Y., Kurosawa, A., & Sekine, M. (2013). Generalized Lyzenga's predictor ofshallowwater depth for multispectral satellite imagery. *Marine Geodesy*, *36(4)*, 365–376.

Kerr, J. M., & Purkis, S. (2018). An algorithm for optically-deriving water depth from multispectral imagery in coral reef landscapes in the absence of ground-truth data. *Remote Sensing of Environment*, *210*, 307–324.

Khondoker, M. S. I., Siddiquee, M., & Hasan, Z. (2016). Deriving River Bathymetry Using Space Borne Remote Sensing Technique in Bangladesh. *IOSR Journal of Engineering (IOSRJEN)*, *1*(1), 45–51. http://article.sciencepublishinggroup.com/pdf/10.11648.j.aos.20160101.12.pdf

Lee, Z., Carder, K. L., Mobley, C. D., Steward, R. G., & Patch, J. S. (1999). Hyperspectral remote sensing for shallow waters: Deriving bottom depths and water properties by optimization. *Applied Optics*, *38*, 3831–3843.

Liang, J., Zhang, J., Ma, Y., & Zhang, C.-Y. (2017). Derivation ofbathymetry fromhigh-resolution optical satellite imagery andUSVsounding data. *Marine Geodesy*, *40(6)*, 466–479.

Lyons, M., Phinn, S., & Roelfsema, C. . (2011). Integrating Quickbird multi-spectral satellite and field data: Mapping bathymetry, seagrass seagrass cover, seagrass species and change in Moreton Bay, Australia in 2004 and 2007. *Remote Sens.*, *3*, 42–64. https://doi.org/https://doi.org/10.3390/rs3010042, 2011.

Lyzenga, D. R. (1981). Remote sensing of bottom reflectance and water attenuation parameters in shallow water using aircraft and Landsat data. *International Journal of Remote Sensing*, *2(1)*, 71–82.

Lyzenga, D. R., Malinas, N. P., & Tanis, F. J. (2006). Multispectral Bathymetry Using a Simple Physically Based Algorithm. *IEEE Transactions on Geosciences and Remote Sensing*, *44*, 2251–2259. http://dx.doi.org/10.1109/TGRS.2006.872909

Lyzenga, D.R. (1978). Passive remote sensing techniques for mapping water depth and bottom features. *Applied Optics*, *17*, 379–383.

Lyzenga, David R. (1985). Shallow-water bathymetry using combined lidar and passive multispectral scanner data. *International Journal of Remote Sensing*, *6*(1), 115–125. https://doi.org/10.1080/01431168508948428

Madricardo, F., Foglini, F., Kruss, A., Ferrarin, C., Pizzeghello, N. M., Murri, C., Rossi, M., Bajo, M., Bellafiore, D., Campiani, E., & Al., E. (2017). High Resolution Multibeam and Hydrodynamic Datasets of Tidal Channels and Inlets of the Venice Lagoon. *Sci. Data*, *4*, 170121.

Maloof, A. C., & Grotzinger, J. P. (2012). The Holocene shallowing-upward parasequence of north-west Andros Island, Bahamas. *Sedimentology*, *59*, 1375–1407.

Mason, D. C., Gurney, C., & Kennett, M. . (2000). Beach Topography Mapping—A Comparison of Techniques. *J. Coast. Conserv*, *6*, 113–124.

Mishra, D., Narumalani, S., Rundqulst, D., & Lawson, M. (2006). Benthic habitat mapping in tropical marine environments using QuickBird multispectral data. *Photogrammetric Engineering & Remote Sensing*, *72*, 1037–1048.

Mohamed, H., Negm, A., Zahran, M., & Saavedra, O. C. (2016). Bathymetry Determination from High Resolution Satellite Imagery Using Ensemble Learning Algorithms in Shallow Lakes: Case Study El-Burullus Lake. *International Journal of Environmental Science and Development*, *7*(4), 295–301. https://doi.org/10.7763/ijesd.2016.v7.787

Ogunkoya, O. O. (2012). All Rivers run into the sea; yet the sea is not full. In *Inaugural lecture Series 256*. Obafemi Awolowo University, Ile Ife Nigeria.

Okolie, C. J. (2015). *Satellite derived bathymetry for hydrographic applications and coastal terrain modelling*. University of Lagos, Nigeria.

Olayinka, D. N., & Okolie, C. J. (2017). Bathymetric Mapping of Nigerian Coastal Waters from Optical Imagery. *Journal of Engineering Research*, *22*(December 2017).

Oyekanmi, M., & Mbossoh, E. R. (2018). Dams and Sustainable Development Goals: A Vital Interplay for Sustainability. *Journal of Environment and Earth Science*, *8*(4), 1-11–11.

Pacheco, A., Horta, J., Loureiro, C., & Ferreira, Ó. (2015). Retrieval of Nearshore Bathymetry from Landsat 8 images: A tool for Coastal Monitoring in Shallow Waters. *Remote Sensing of Environment*, *159*, 102–116.

Park, J. Y., Ramnath, V., Feygels, V., Kim, M., Mathur, A., Aitken, J., & Tuell, G. (2010). Active-Passive Data Fusion Algorithms for Seafloor Imaging and Classification from CZMIL Data. *SPIE Proceedings on Algorithms and Technologies for Multispectral, Hyperspectral, and Ultraspectral Imagery*. https://doi.org/doi:10.1117/12.851991

Pastol, Y. (2011). Use of Airborne LIDAR Bathymetry for Coastal Hydrographic Surveying: The French Experience. *Journal of Coastal Research: Special*, *62*, 6 – 18.

Philpot, W. D. (1989). Bathymetric mapping with passive multispectral imagery. *Applied Optics*, *28*, 1569 – 1578.

Porskamp, P., Rattray, A., Young, M., & Ierodiaconou, D. (2018). Multiscale and Hierarchical Classification for Benthic Habitat Mapping. *Geosciences*, *8*, 119.

Salameh, E., Frappart, F., Almar, R., Baptista, P., Heygster, G., Lubac, B., Raucoules, D., Almeida, L. P., Bergsma, E. W. J., Capo, S., De Michele, M. D., Idier, D., Li, Z., Marieu, V., Poupardin, A., Silva, P. A., Turki, I., & Laignel, B. (2019). Monitoring Beach Topography and Nearshore Bathymetry Using Spaceborne Remote Sensing: A Review. *Remote Sensing*, *11*(19). https://doi.org/10.3390/rs11192212

Sam, L., Prusty, G., & Gahlot, N. (2018). Evaluation of optical remote sensing-based shallow water bathymetry for recursive mapping. *Geocarto International*, *33*(7), 737–753. https://doi.org/10.1080/10106049.2017.1299800

Stumpf, R. P., Holderied, K., & Sinclair, M. (2003). Determination of water depth with high-resolution satellite imagery over variable bottom types. *Limnology and Oceanography*, *48*(1 II), 547–556. https://doi.org/10.4319/lo.2003.48.1_part_2.0547

Su, H., Liu, H., & Heyman, W. (2008). Automated derivation for bathymetric information for multispectral satellite imagery using a non-linear inversion model. *Marine Geodesy*, *31*, 281–298.

Su, Haibin, Liu, H., & Heyman, W. (2008). Automated derivation of bathymetric information from multi-spectral satellite imagery using a non-linear inversion model. *Marine Geodesy*, *31*(4), 281–298. https://doi.org/10.1080/01490410802466652

Taiwo, A. A., Adebukola, A. A., Adedeji, I. A., & Yetunde, F. T. (2017). Effect of discharges from re-channeled rivers and municipal runoff on water quality of Opa reservoir, Ile-Ife, Southwest Nigeria. *African Journal of Environmental Science and Technology*, *11*(1), 56–70. https://doi.org/10.5897/ajest2016.2086

Tuell, G. H., Ramnath, V., Park, J. Y., Feygels, V., Aitken, J., & Kopelivich, Y. (2005). Fusion of SHOALS bathymetric LIDAR and passive spectral data for shallow water rapid environmental assessment. *Proceedings of the Oceans*, *2*, 1046–1051.

Vinayaraj, P., Raghavan, V., & Masumoto, S. (2016). Satellite-Derived Bathymetry using Adaptive Geographically Weighted Regression Model. *Marine Geodesy*, *39*(6), 458–478. https://doi.org/10.1080/01490419.2016.1245227

Vogelzang, J., Wensink, G. J., De Loop, G. P., Peters, H. C., & Pouwels, H. (1943). Sea Bottom Topography with X-Band SLAR: The Relation between Radar Imagery and Bathymetry. *International Journal of Remote Sensing*, *13*, 1943–1958. https://doi.org/http://dx.doi.org/10.1080/01431169208904242

Wang, C. K., & Philpot, W. D. (2007). Using airborne bathymetric lidar to detect bottom type variation in shallow waters. *Remote Sensing of Environment*, *106*, 123–35.

Yunus, A. P., Dou, J., Song, X., & Avtar, R. (2019). Improved bathymetric mapping of coastal and lake environments using sentinel-2 and landsat-8 images. *Sensors (Switzerland)*, *19*(12), 1–19. https://doi.org/10.3390/s19122788

BIOGRAPHICAL NOTES

Caleb Oluwadare is a Senior Lecturer and the acting Head in the Department of Surveying and Geoinformatics, Obafemi Awolowo University Ile-Ife, Nigeria. He is a Registered Surveyor and a Member of the Nigerian Institution of Surveyors. He holds a Doctor of Philosophy Degree in Geography, M. Sc. (Remote Sensing and Geographic Information System), B.Sc. (Surveying, Geodesy and Photogrammetry). His work centres on Land administration and GIS applications.

Email: **coluwadare@oauife.edu.ng**
Mobile: +2348035920575

Emmanuel Tolulope SANYAOLU is a Technologist I in the Department of Surveying and Geoinformatics, Obafemi Awolowo University Ile-Ife, Nigeria. He is a Registered Surveyor.

He holds a Post Graduate Diploma in Geographic Information Production and Management, B.Sc. & H.N.D. (Surveying, and Geoinformatics). He possesses the technical skills in handling Remote Sensing and GIS analysis using software such as QGIS, ILWIS, ArcGIS, IDRISI, Google Earth Engine, Envi, etc. His area of research interest includes Hydrographic Surveying, Remote Sensing and Geographic Information System (GIS).

Email: ***sanyaoluet@oauife.edu.ng***

Mobile: +2348057882827